https://doi.org/10.5194/egusphere-2026-6827
Preprint. Discussion started: 19 November 2026
© Author(s) 2026. CC BY 4.0 License.

Alkalinity loss and limited ecological responses in a trio of tropical coastal ocean alkalinity enhancement experiments

Xuechao Wang[1,2], Yuanhao Liu[1], Apsara Patteri Vijayan[1], Ruqin Bai[1], Ruoyu Niu[1], Qixing Ji[3], Gang Li[4], Shengwei Hou*[1], and Mark James Hopwood*[1]

[1]Department of Ocean Science and Engineering, Southern University of Science and Technology, Shenzhen 518055, China
[2]Institute of Marine Science and technology, Shandong University, Qingdao 266237, China.
[3]Earth, Ocean and Atmospheric Sciences Thrust, The Hong Kong University of Science and Technology (Guangzhou), Guangzhou 511453, China
[4]Daya Bay Marine Biology Research Station, South China Sea Institute of Oceanology, Chinese Academy of Sciences, Guangzhou, 510530, China

Correspondence to: Mark James Hopwood (mark@sustech.edu.cn) and Shengwei Hou (housw@sustech.edu.cn)

Abstract. The Ocean Alkalinity Enhancement Pelagic Impact Intercomparison Project (OAEPIIP) defines common CO_2-unequilibrated and CO_2-equilibrated scenarios to systematically test the pelagic effects of OAE using sodium hydroxide (NaOH) worldwide. Two key uncertainties in the application of OAE to coastal systems are whether the carbonate chemistry and ecological responses to alkalinity additions remain comparable between inshore and offshore waters. Inshore, and particularly estuarine, environments are more susceptible to loss of alkalinity from heterogeneous precipitation of calcium carbonate. Similarly, inshore pCO_2 and pH dynamics are typically more spatially and temporally variable than offshore systems, such that inshore ecosystems may be less sensitive to pH perturbations from OAE. Critically, the NaOH doses applied in the OAEPIIP protocol were intended to be sufficiently low to exclude the possibility of calcium carbonate precipitation and significant ecological effects. Here we ran three simultaneous 20-day OAEPIIP experiments using estuarine, inner bay and offshore seawater from Daya Bay (Guangdong, China) during a diatom bloom. In all three cases, there was no clear evidence for responses of bulk biomass, nutrients, biogenic silica, nitrous oxide (N_2O), methane (CH_4), or prokaryotic communities to NaOH addition. Phytoplankton exhibited some modest, taxon-specific responses to NaOH addition. All equilibrated treatments approached the intended +500 µmol kg^{-1} total alkalinity (TA) increase. However, TA concentrations in unequilibrated treatments were only +149 to +253 µmol kg^{-1} above control treatments on Day 20. This result was reproducible between replicate treatments and resembles the apparent TA loss reported in other regional OAE experiments using both NaOH and

https://doi.org/10.5194/egusphere-2026-6827
Preprint. Discussion started: 19 November 2026
© Author(s) 2026. CC BY 4.0 License.



$Mg(OH)_2$ as alkalinity sources. Whilst not explicitly confirmed, as OAEPIIP was designed with an assumption that TA loss would not be observed, these results implicate heterogeneous alkalinity loss as a key concern for OAE deployment in this environmental context.

1 Introduction

Ocean alkalinity enhancement (OAE) is a proposed marine carbon dioxide removal strategy that increases seawater alkalinity to enhance oceanic CO_2 uptake and long-term carbon storage as dissolved inorganic carbon (DIC) (Eisaman et al., 2023; Hartmann et al., 2013; Kheshgi, 1995; Renforth and Henderson, 2017). As OAE research moves from theoretical assessment to experimental evaluation and field trials, potential ecological and biogeochemical consequences need to be constrained under environmentally realistic conditions (Bach et al., 2019; Gattuso et al., 2021; Riebesell et al., 2023). In pelagic systems, this includes evaluating potential changes to plankton, organic carbon and nutrient dynamics, and the biogeochemistry of other greenhouse gases (e.g. N_2O and CH_4). Investigations constraining the environmental effects of OAE not only aim to exclude the possibility of unexpected or detrimental ecological effects, but also to constrain potential additionalities which affect the overall net carbon sequestration potential of OAE deployment (Bach, 2023).

In pelagic systems, a particularly critical difference arises between whether alkalinity additions to achieve OAE are 'equilibrated' or 'unequilibrated' with respect to ambient pCO_2. Unequilibrated alkalinity additions to seawater temporarily increase pH, decrease dissolved CO_2, and increase calcium carbonate saturation states. These chemical perturbations may affect some marine organisms (He and Tyka, 2022; Renforth and Henderson, 2017; Schulz et al., 2023). Conversely, equilibrated alkalinity additions have only minor effects on ambient carbonate chemistry as alkalinity is added to seawater after pre-reaction with CO_2. Biogeochemical responses to OAE are therefore expected to differ between equilibrated and unequilibrated scenarios, rather than depending solely on the alkalinity dosage applied (Ferderer et al., 2022; Kousoulas et al., 2025; Ramírez et al., 2025). Accordingly, this distinction is a major consideration in the OAEPIIP experiment design (Bach, 2024). A key hypothesis across the whole OAEPIIP project is that ecological responses, if present, are more likely in response to unequilibrated NaOH additions.

Whilst an increasing body of literature has assessed the potential impacts of OAE on pelagic ecology (Sánchez et al., 2024; Tammen et al., 2026; Xin et al., 2024), numerous alkalinity sources and doses have been considered which often precludes direct comparisons of the ecological responses to OAE between regions. Prior work in the East and South China Sea, for example, has used a mixture of alkalinity sources including $Mg(OH)_2$ and olivine (Liu et al., 2026; Zhang et al., 2026). A standardised framework, such as OAEPIIP, improves inter-region and inter-experiment comparability by defining common manipulation procedures and treatment targets (Bach et al., 2024). The realised carbonate chemistry perturbation, biological context, and response pathways can thereby be reported together and directly compared to other regional contexts (Bach et al., 2026). Without this direct inter-comparability, it is challenging to conclusively distinguish between different ecological

https://doi.org/10.5194/egusphere-2026-6827
Preprint. Discussion started: 19 November 2026
© Author(s) 2026. CC BY 4.0 License.

sensitivities to OAE, dose-dependent trajectories, alkalinity source-dependent trajectories, and other method specific effects (Boyd et al., 2019).

Here, we use a trio of OAEPIIP experiments conducted across a tropical bay to test the ecological and biogeochemical responses of CO_2-unequilibrated and CO_2-equilibrated exposure scenarios in a coastal pelagic system. We compare three source-water localities spanning estuarine, inner bay, and offshore conditions.

2 Materials and methods

2.1 Study site and experimental setup

All experiments were conducted in Daya Bay (Guangdong, China) in the northern part of the South China Sea, during the dry season in boreal winter (December 2024–January 2025). Surface seawater was collected on 23 December 2024 from three locations that were operationally defined as 'Estuary', 'Inner Bay', and 'Offshore' source waters, based on their geographic setting (Figure 1). All source-water collection was completed within one day. The 55 L PET FermZilla microcosms were filled directly by submerging from a small boat with the engine switched off. The incubators were pre-cleaned with seawater, then opened at both ends, submerged below the surface, sealed, shaded with black plastic and returned to a coastal laboratory.

At the initial sampling point, temperature was similar among the three source waters (Estuary: 17.0–17.7 °C; Inner Bay: 16.7–17.8 °C; Offshore: 17.2–17.7 °C). Salinity ranged from 31.04 to 32.09 in the Estuary, 31.69 to 32.03 in the Inner Bay, and 30.66 to 32.31 in the Offshore source water. The salinity gradient across the bay was minimal as sampling was conducted during the dry season. A total of 27 incubators were used, comprising three source-water groups with nine incubators per group. Within each source-water group, three treatments were established with triplicate biological replicates per treatment. The experimental design followed the standard OAEPIIP framework (Bach et al., 2024). The Daya Bay experiment therefore represents a local implementation of the standardised OAEPIIP pelagic microcosm protocol across contrasting coastal water masses.

After returning ashore, 55 L incubators were transported to an insulated room pre-prepared with a homogenized light regime. The mass of each incubator was compared to its pre-determined dry weight to obtain the specific mass of seawater in each individual incubator. Incubators were orientated in 3 rows under strip full-spectrum LED grow light (42 W; Barrina) arranged to produce the same light exposure to all incubators. The temperature of the room was set to 17°C to approximate *in situ* conditions. One aspect of the standardized OAEPIIP experiment design was altered following a pre-experiment trial. The standard design uses belt heaters on the outside of incubators. However, excessive numbers of belt heaters were found to make it challenging to control the temperature of the room as the majority of heat from these heat sources is radiated into the room. Therefore, belt heaters were replaced with 200 W aquarium heaters (Sensen) positioned inside each incubator and set at 18°C. Aquarium heaters were pre-soaked in deionized water while heating for 2 days, then one heater was positioned at the base of each 55 L incubator to induce convective mixing as per the belt heaters.

https://doi.org/10.5194/egusphere-2026-6827
Preprint. Discussion started: 19 November 2026
© Author(s) 2026. CC BY 4.0 License.

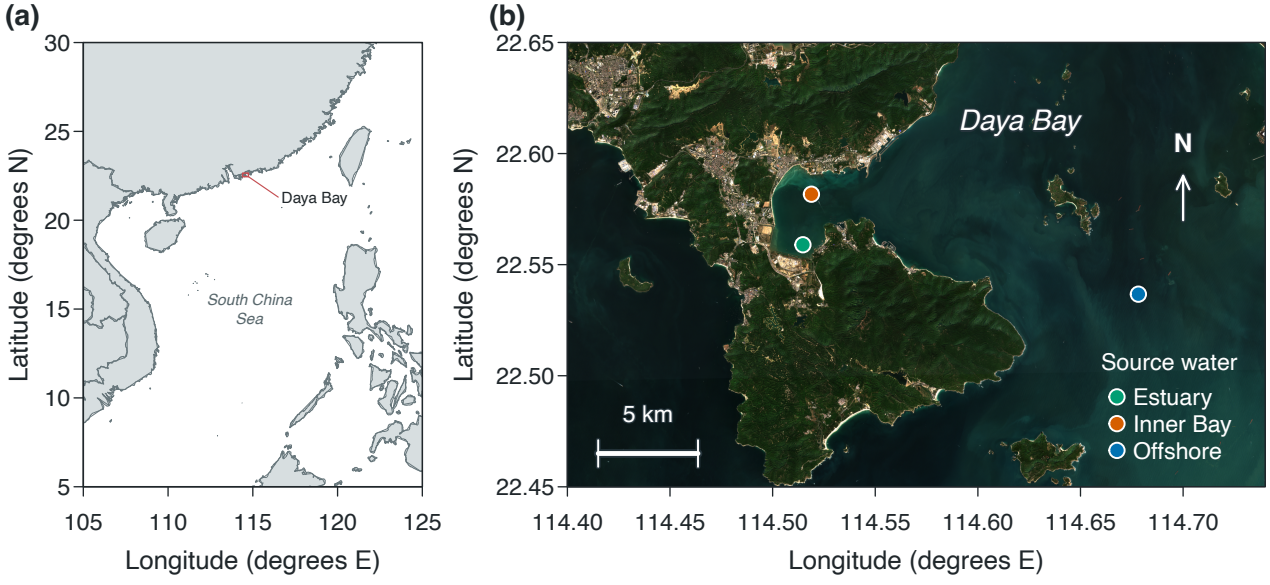


Figure 1. Sampling locations for the Daya Bay OAEPIIP experiments. (a) Regional position of Daya Bay in the northern South China Sea. (b) Sentinel-2 true-colour composite showing the source-water sampling locations: Estuary (green), Inner Bay (orange) and Offshore (blue). Surface seawater collected from each source-water type was distributed into 9 sets of 55 L PET FermZilla microcosm containers for the control, CO_2-unequilibrated OAE, and CO_2-equilibrated OAE treatments.

2.2 Definition of equilibrated and unequilibrated OAE treatments

Treatments were designed to distinguish between an unequilibrated OAE state and an equilibrated OAE state pre-treated with CO_2. This distinction follows the standardized OAEPIIP protocol (Bach et al., 2024) and is treated here as the primary contrast of interest for response interpretation. Three treatments were thereby established for each of the three source waters: a control without alkalinity manipulation, a CO_2-unequilibrated OAE scenario, and a CO_2 equilibrated OAE scenario. The two OAE scenarios followed the standard OAEPIIP +500 µmol kg^{-1} TA dosage.

In the unequilibrated treatment, alkalinity was increased by addition of 1 M NaOH without a corresponding initial increase in DIC, thereby producing the immediate post-addition OAE state characterised by elevated TA, reduced pCO_2, and altered DIC speciation. In the equilibrated treatment, seawater was manipulated to approximately represent the post-gas-exchange OAE state, such that alkalinity enhancement was accompanied by a corresponding increase in DIC and seawater pCO_2 remained near atmospheric equilibrium. The manipulation scheme followed the OAEPIIP protocol described by Bach et al. (2024), with the reagent specifications and actual addition volumes used in this study are detailed below.

The NaOH stock was a commercially supplied 1.0 M standard solution (BKMAN). The 1.0 M $NaHCO_3$ stock solution was prepared from sodium bicarbonate (MACKLIN; 99.9% pure trace metal grade). The entire dosing procedure was completed within 15 min. Initial TA and DIC for calculations were estimated from observed salinity and prior observations in the bay as doses had to be applied immediately after water was returned to the laboratory. Dose calculations assumed an initial TA of 2250 µmol kg^{-1} and a target increase of 500 µmol kg^{-1}, corresponding to a target TA of 2750 µmol kg^{-1}. The required additions

https://doi.org/10.5194/egusphere-2026-6827
Preprint. Discussion started: 19 November 2026
© Author(s) 2026. CC BY 4.0 License.

were calculated using the actual salinity, seawater mass (from weighing each individual incubator), and other relevant parameters for each microcosm (Table 1).

Table 1 Recorded seawater masses and volumes of 1 M stock solutions added to individual microcosms.

Source water	Treatment	Replicate	Seawater mass (kg)	NaOH (mL)	$NaHCO_3$ (mL)	Nominal ΔTA (μmol kg^{-1})
Estuary	Control	1	55.85			
Estuary	Control	2	55.30			
Estuary	Control	3	55.65			
Estuary	Equilibrated	1	53.80	4.055	22.845	500
Estuary	Equilibrated	2	53.15	4.006	22.569	500
Estuary	Equilibrated	3	54.80	4.131	23.270	500
Estuary	Unequilibrated	1	54.10	27.050		500
Estuary	Unequilibrated	2	51.70	25.850		500
Estuary	Unequilibrated	3	54.95	27.475		500
Offshore	Control	1	55.85			
Offshore	Control	2	52.75			
Offshore	Control	3	55.60			
Offshore	Equilibrated	1	54.15	4.092	22.983	500
Offshore	Equilibrated	2	53.80	4.065	22.835	500
Offshore	Equilibrated	3	53.50	4.042	22.708	500
Offshore	Unequilibrated	1	55.75	27.880		500
Offshore	Unequilibrated	2	58.30	29.150		500
Offshore	Unequilibrated	3	53.40	26.700		500
Inner Bay	Control	1	55.05			
Inner Bay	Control	2	53.65			
Inner Bay	Control	3	53.05			
Inner Bay	Equilibrated	1	54.45	4.101	23.124	500
Inner Bay	Equilibrated	2	53.75	4.048	22.827	500
Inner Bay	Equilibrated	3	55.50	4.180	23.570	500
Inner Bay	Unequilibrated	1	54.35	27.175		500
Inner Bay	Unequilibrated	2	51.80	25.900		500
Inner Bay	Unequilibrated	3	53.60	26.800		500

https://doi.org/10.5194/egusphere-2026-6827
Preprint. Discussion started: 19 November 2026
© Author(s) 2026. CC BY 4.0 License.

2.3 Carbonate chemistry measurements and calculations

Salinity and temperature were measured at each sampling point using an EXO1 multiparameter probe (YSI, USA) inserted directly into each experimental container. Across all incubation bottles and sampling days, measured water temperature averaged 17.35 ± 1.00 °C (mean ± standard deviation). Experimental containers were arranged before the experiment so that source-water groups, treatments, and biological replicates were distributed across the experimental area in pre-marked orientations with equal light exposure. Incubations were maintained under a 12:12 h light:dark cycle. Light intensity at the water surface was measured daily using a photosynthesis light quantum meter (TES 1399P), and the distance between the lamps and incubation bottles was adjusted as the water level declined to maintain surface irradiance at 200 ± 10 µmol photons m^{-2} s^{-1}.

For TA, pH and DIC measurements, 250 mL of seawater was gently sampled from below the surface into pre-rinsed 250 mL borosilicate glass bottles (Corning). Samples were sealed with greased stoppers (Apiezon L-Grease) and stored in cool boxes in the dark until same-day analysis. TA was measured by open-cell titration using an Apollo AS-ALK2 titrator (Apollo SciTech Inc.) equipped with a high-precision pH meter (Orion Star A211 Benchtop, Thermo Scientific). Each sample was measured in duplicate, and a third replicate was analysed if duplicates differed by >10 µmol kg^{-1}. The pH electrode was calibrated daily using National Bureau of Standards buffers (pH 4, 7, and 10), and electrodes were used only when calibration yielded a slope >95 %. All titrations were conducted at 25 °C in a temperature-controlled water bath (DC-1010, SCIENTZ). Certified reference material (from Prof. A. Dickson, Scripps Institution of Oceanography, USA; batch #200) was analysed regularly during sample runs (measured: 2190 ± 7 µmol kg^{-1}, n = 58; certified: 2186.43 ± 0.42 µmol kg^{-1}). DIC was measured using an Apollo AS-C5M DIC Analyzer (Apollo SciTech Inc.). Samples were analysed in batches of eight following calibration with the same certified reference material, yielding reproducibility better than 0.2 %. TA, DIC, temperature, and salinity were used to calculate other carbonate system parameters with CO2SYS (Pierrot et al., 2021), using the carbonic acid dissociation constants of Lueker et al. (2000), $KHSO_4$ from Dickson (1990), borate constants from Lee et al. (2010), and HF from Perez and Fraga (1987).

2.4 Biological and biogeochemical response variables

Samples for other parameters were collected by siphoning while gently agitating the incubators. For chlorophyll-a analysis, 250 mL of seawater was filtered through GF/F filters within 2 h of sampling. Filters were stored at −20 °C until extraction in 10 mL 90 % acetone for 24 hours at −20 °C in the dark. Chlorophyll-a fluorescence was then measured using a Trilogy Laboratory Fluorometer (Turner Designs) following Welschmeyer (1994). Chlorophyll-a was used as the primary bulk-biomass response variable.

Phytoplankton populations were analysed using a FACSAria II flow cytometer (BD Biosciences, USA). Seawater aliquots (1.8 mL) were fixed with 20 µL of 50% glutaraldehyde for 15–20 min in the dark. Samples were flash-frozen in liquid nitrogen and stored at −20 °C during the experiment. Following completion of the incubations, samples were transported to the

https://doi.org/10.5194/egusphere-2026-6827
Preprint. Discussion started: 19 November 2026
© Author(s) 2026. CC BY 4.0 License.

laboratory and stored at −80 °C until analysis. Photosynthetic events were identified using red chlorophyll autofluorescence and side scatter, with forward scatter and orange fluorescence used for further discrimination. A consistent gating scheme distinguished three operational groups: Pico, phycoerythrin-rich Synechococcus-like cells (Syn), and nanophytoplanton (Nano) populations. Abundances were calculated from gated event counts and effective analysed volumes, using the calibrated flow rate (28.0 µL per 180 s) and FCS-recorded acquisition duration. Three initial source-water samples provided a shared pre-addition baseline for all treatments within each experiment.

Samples for dissolved inorganic nitrate plus nitrite (NO_x^-), dissolved inorganic phosphate (DIP), and dissolved silicic acid were syringe-filtered through 0.22 µm filters (Millipore) into 50 mL polypropylene tubes (Fisherbrand). Hereafter, NO_x^- denotes nitrate plus nitrite, PO_4^{3-} denotes phosphate, and $Si(OH)_4$ denotes dissolved silicic acid. Concentrations of $Si(OH)_4$ were measured within 1 d of sample collection, whereas NO_x^- and PO_4^{3-} samples were frozen at −20 °C until analysis at the end of the experiment. Nutrient concentrations were determined spectrophotometrically following Grasshoff et al. (1983), with daily instrument calibration and detection limits defined as three times the standard deviation of deionized-water blank measurements performed after every 10 samples. Detection limits (mean ± 1 SD) were 0.06 ± 0.02 µmol L^{-1} for PO_4^{3-}, 0.15 ± 0.02 µmol L^{-1} for NO_x^-, and 0.10 ± 0.06 µmol L^{-1} for $Si(OH)_4$.

Biogenic silica (BSi) was determined following the alkaline extraction method of DeMaster (1981). A 400 mL water sample was filtered through a 0.8 µm polycarbonate filter (Whatman), which was stored at −20 °C until analysis. For digestion, each filter was placed in a 50 mL vial containing 25 mL of 0.1 M Na_2CO_3 solution and incubated at 85 °C. Aliquots of the extract were collected after 1, 2, 3, and 5 h. Depending on the dilution required, either 500 or 800 µL of each aliquot was diluted to a final volume of 10 mL with deionised water and then neutralised with HCl. Dissolved silica concentrations were then determined using a UV–Vis spectrophotometer 8000 (Metash Instruments Co., Ltd., Shanghai, China), following Grasshoff (1983). Dissolved silica concentration was plotted against extraction time, and the intercept obtained by extrapolation to zero time was used to estimate BSi content. Blank values were determined using filters rinsed with deionised water and processed following the same procedure.

Dissolved N_2O and CH_4 were sampled on experimental Days 0, 1, 4, 12, 16, and 20. Samples were collected by siphoning water from the middle of each 55 L incubation bottle into 20 mL serum bottles (Anpel Laboratory Technologies, Shanghai, China). Each bottle was allowed to overflow during filling, and duplicate samples were collected from each microcosm. Immediately after sampling, samples were preserved with 0.1 mL of 10 M NaOH to inhibit bacterial activity (Frey et al., 2024), and then sealed with rubber septa and aluminium crimp caps. Dissolved N_2O and CH_4 were measured by headspace equilibration followed by gas chromatography using an electron capture detector and flame ionisation detector (Asicotech M6, Shanghai, China), following Chen et al. (2025b). Analytical precision was better than 3% relative standard deviation. Dissolved gas concentrations were calculated from headspace partial pressures using published solubility-based approaches for N_2O and CH_4 (Goreau et al., 1980; Kozlowski et al., 2014).

https://doi.org/10.5194/egusphere-2026-6827
Preprint. Discussion started: 19 November 2026
© Author(s) 2026. CC BY 4.0 License.

2.5 Microbial community composition

For microbial community composition, microbial biomass was collected at the start and end of the incubation. On Day 0, 2 L of source seawater was filtered from triplicate initial samples during microcosm filling. On Day 20, 2 L of seawater was siphoned from the middle of each incubation bottle and filtered through 0.22 µm Sterivex filter units (Millipore, USA). Filters were opened aseptically, and DNA was extracted using the FastDNA SPIN Kit for Soil (MP Biomedicals, USA) following the manufacturer's protocol. The 515Y and 926R primers were used to amplify prokaryotic 16S and eukaryotic 18S rRNA gene regions, and the PCR workflow follows Yeh et al. (2021) and McNichol et al. (2021). Sequencing was performed on an Illumina NovaSeq 6000 platform in paired-end 250 bp mode (PE250).

Amplicon data were processed in QIIME2 v2024.02 (Bolyen et al., 2019) using the Fuhrman laboratory eASV workflow (Yeh et al., 2021), except for the taxonomic annotation of eukaryotic microbes. Briefly, Cutadapt was used for demultiplexing and primer trimming (Martin, 2011), BBSplit (BBTools version 39.19, https://sourceforge.net/projects/bbmap/) was used to separate prokaryotic and eukaryotic reads, and DADA2 (v1.26.0) was used for denoising, paired-end merging, and amplicon sequence variant (ASV) inference (Bolyen et al., 2019; Callahan et al., 2016). Taxonomy was assigned with SILVA 138.1, and ASVs assigned to chloroplasts or mitochondria were removed (Quast et al., 2012). Samples were rarefied to 72,205 prokaryotic reads before diversity analyses.

The chloroplast reads removed from the prokaryotic table were re-annotated against PR2 v5.1.1 (Guillou et al., 2012) to characterise chloroplast-associated phytoplankton lineages. Taxa were retained with the ":plas" suffix to distinguish chloroplast from nuclear 18S assignments; Streptophyta annotations were removed (Junger et al., 2026), and samples were rarefied to 3,856 reads. The eukaryotic reads were trimmed and merged with BBMap (BBTools version 39.19, https://sourceforge.net/projects/bbmap/), denoised with DADA2's single-end workflow (Callahan et al., 2016), and annotated against PR2 v5.1.1 (Guillou et al., 2012). Metazoa, Streptophyta and sequences containing "nucl" (nucleomorph) in the annotation were removed (Junger et al., 2026), and samples were rarefied to 408 reads. Taxonomic annotation of both chloroplast and eukaryotic sequences was performed using VSEARCH (v2.32.0, --sintax_cutoff 0.8, --sintax_random, --randseed 42) (Rognes et al., 2016). Relative-abundance patterns from these low-depth 18S data were interpreted as exploratory taxonomic responses.

2.6 Statistical analyses

Treatment trajectories for TA, DIC, pH and chlorophyll-a were analysed using generalized additive mixed models (GAMMs), with source-water type and treatment represented as a combined factor, experimental day fitted using treatment-specific smooth terms, and bottle identity included as a random intercept. Chlorophyll-a concentrations were log-transformed before analysis. Models were fitted to observations from experimental Days 1–20; Day 0 measurements were retained as a common pre-addition reference but were not included in the post-addition trajectory fits. Treatment contrasts between CO_2-equilibrated and CO_2-unequilibrated treatments were estimated within each source-water type with approximately 95% simultaneous

https://doi.org/10.5194/egusphere-2026-6827
Preprint. Discussion started: 19 November 2026
© Author(s) 2026. CC BY 4.0 License.

confidence intervals. Other response variables were evaluated from their observed treatment trajectories and source-water patterns.

Microbial Simpson diversity, non-metric multidimensional scaling (NMDS), and analysis of similarity (ANOSIM) were calculated in R (v4.2.3, Team, 2023) using vegan (v2.6-4) and phyloseq (v1.42.0) (McMurdie and Holmes, 2013; Oksanen et al., 2022). Putative metabolic functions were inferred with FAPROTAX (v1.2.12) (Louca et al., 2016). Because microbial DNA samples were available only for the initial and final time points, these data were used to assess broad community-level consistency with the carbonate-chemistry separation rather than to resolve within-incubation temporal dynamics.

3 Results

The series of three OAEPIIP incubations from three source waters were completed in parallel over 20 days. Whilst the incubators represent open systems, as the lids were secured ajar in order to facilitate air exchange, the salinity changes observed over the experiment duration were minor or negligible. Mean salinity was 31.92 ± 0.45 on Day 0 and 31.97 ± 0.22 on Day 20 (mean ± SD; $n \geq 26$ at each time point). Therefore, we discuss TA dynamics in terms of absolute concentrations without any corrections for net evaporation. One 55 L incubator was removed from the Estuary equilibrated experiment after Day 1 because of a malfunctioning heater which corroded and likely contaminated the water. All other observations proceeded as planned.

3.1 OAEPIIP scenarios produced distinct carbonate chemistry trajectories

Alkalinity addition elevated TA in both OAE treatments relative to the contemporaneous controls across all three source-water types (Figure 2a–c). In the equilibrated treatment, TA enhancement was +396 to +474 µmol kg^{-1} on Day 1 (Inner Bay: +474; Estuary: +396; Offshore: +474 µmol kg^{-1}) and +488 to +500 µmol kg^{-1} on Day 20. These values approached the intended OAEPIIP increase of +500 µmol kg^{-1}. The propagated analytical uncertainty of a TA difference comparing two measured concentrations (e.g. comparing a treatment to the corresponding locality's control) was approximately 10 µmol kg^{-1}.

The unequilibrated treatment retained substantially less dissolved TA. Its enhancement relative to the contemporaneous controls peaked at +212 to +315 µmol kg^{-1} during Days 1–3 and declined to +149 to +253 µmol kg^{-1} by Day 20 (Estuary: +149; Inner Bay: +174; Offshore: +253 µmol kg^{-1}). This pattern was observed in all three source-water types. The GAMMs confirmed that TA remained consistently lower in the unequilibrated than in the equilibrated treatment throughout the Day 1–20 prediction period, with the estimated Day 20 differences ranging from −336 to −247 µmol kg^{-1}.

On Day 1, DIC was 297–386 µmol kg^{-1} higher in the equilibrated than in the unequilibrated treatment, while pH was 0.261–0.311 units higher in the unequilibrated treatment (Figure 2d–i). The pH separation increased during the first week, reaching 0.311–0.358 units, and remained elevated within 0.22–0.26 units on Day 20. The observed Day 20 DIC differences between equilibrated and unequilibrated treatments were 429, 396 and 386 µmol kg^{-1} for Estuary, Inner Bay and Offshore, respectively. GAMM estimates likewise showed persistent DIC and pH separation across all three source-water types. Thus, the two

https://doi.org/10.5194/egusphere-2026-6827
Preprint. Discussion started: 19 November 2026
© Author(s) 2026. CC BY 4.0 License.

OAEPIIP scenarios generated distinct and persistent carbonate-chemistry trajectories, while the magnitude of TA enhancement remained source-water dependent.

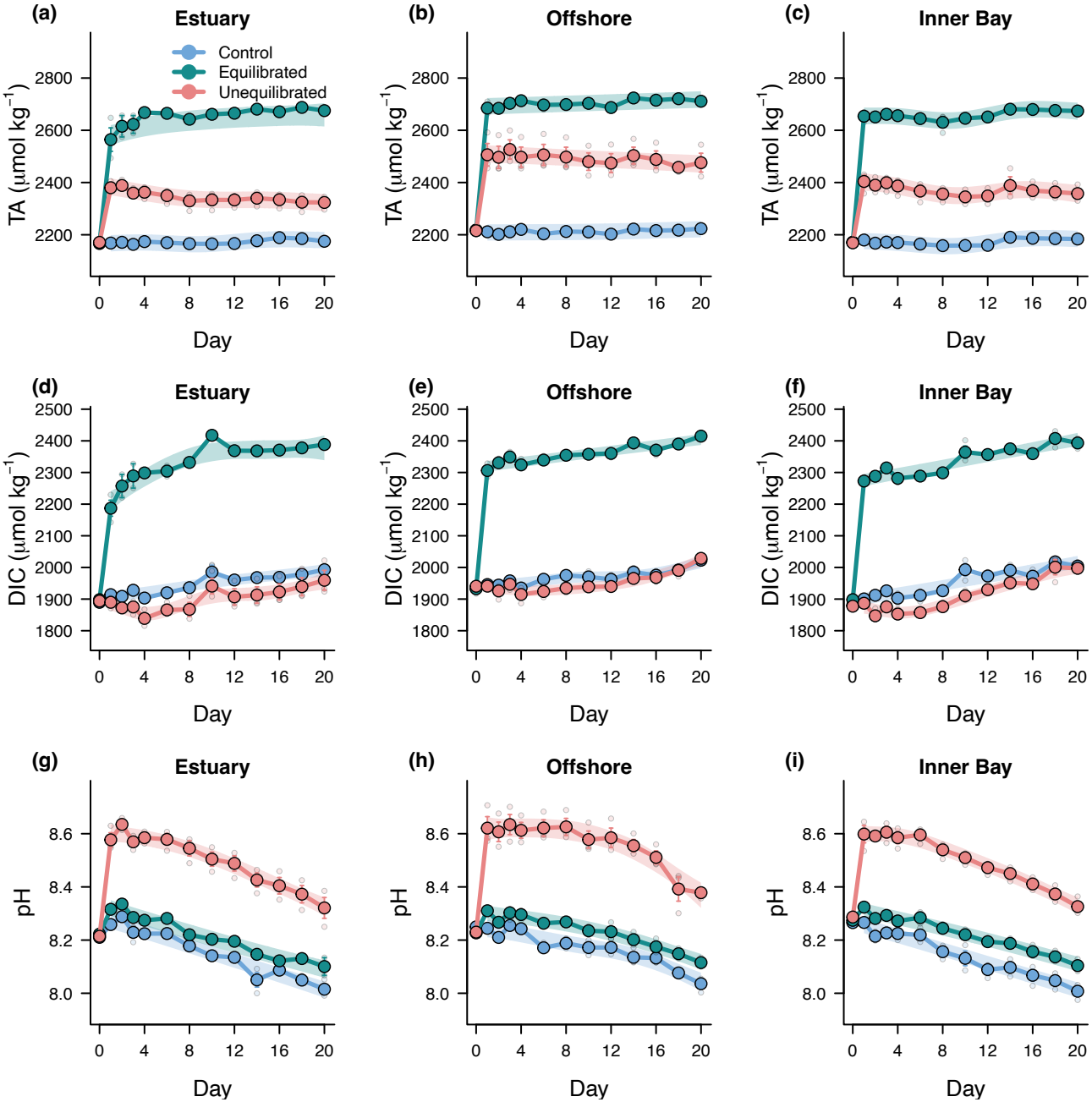


Figure 2. Temporal changes in carbonate chemistry across the three source-water experiments. Panels show total alkalinity (TA; a–c), dissolved inorganic carbon (DIC; d–f), and pH (g–i), with columns representing Estuary, Offshore, and Inner Bay, respectively. Small translucent points represent individual biologically independent microcosms, whereas coloured circles and solid lines show observed treatment means (the individual points are often hidden due to small variability between replicates). Error bars indicate

https://doi.org/10.5194/egusphere-2026-6827
Preprint. Discussion started: 19 November 2026
© Author(s) 2026. CC BY 4.0 License.

±1 standard error where at least two replicates were available; some error bars are smaller than the symbols. Each treatment comprised up to three biological replicates per sampling day. Coloured ribbons show 95% pointwise confidence intervals for population-level mean trajectories estimated using generalised additive mixed models (GAMMs). Day 0 represents pre-addition conditions and is displayed for reference; GAMMs were fitted only to post-addition observations from Days 1–20.

3.2 Ecological responses showed limited divergence across OAE exposure scenarios

Daya Bay is a productive marine environment, with substantial phytoplankton biomass and primary production year-round supported by a combination of sustained terrestrial nutrient inputs and coastal upwelling (Song et al., 2004; Wang et al., 2018; Yang et al., 2020). Diatoms typically dominate the phytoplankton community in Daya Bay and are frequently associated with phytoplankton blooms (Wang et al., 2006; Yang et al., 2020). High chlorophyll-a and high BSi concentrations were consistently observed at the start of all three incubations indicating that a large diatom bloom was underway when the experiment was initiated which is a common regional occurrence. NO_x^- and $Si(OH)_4$ concentrations were relatively low on Day 0, indicating that the *in situ* bloom was likely close to peaking. Days 1-4 were consistently characterised by a rapid decline in chlorophyll-a and BSi in all three experiments, corroborating the end phase of a diatom bloom. NO_x^- and $Si(OH)_4$ concentrations remained within relatively narrow ranges in all three cases. PO_4^{3-} was low and often close to, or below, the detection limit so PO_4^{3-} trends are not interpreted further herein.

NO_x^- and silica-related variables showed a similar pattern: temporal variability and source-water differences were more apparent than a consistent separation between equilibrated and unequilibrated OAE scenarios (Figure 3). NO_x^- varied through time in all three source waters, with some short-lived mid-incubation increases but no persistent ordering of the two OAE scenarios (Figure 3a–c). These patterns indicate that dissolved inorganic nutrient dynamics were not consistently aligned with the carbonate-chemistry contrast between equilibrated and unequilibrated scenarios.

Dissolved silicic acid showed a clearer source-water signal than either NO_x^- or PO_4^{3-} (Figure 3g–i). $Si(OH)_4$ was generally higher and more variable in the Offshore experiment, frequently ranging between approximately 2 and 4 μmol L^{-1}, whereas the Inner Bay experiment generally remained lower and showed a narrower range for much of the incubation. This suggests that $Si(OH)_4$ dynamics were more strongly structured by source-water context and temporal change than by exposure scenario.

https://doi.org/10.5194/egusphere-2026-6827
Preprint. Discussion started: 19 November 2026
© Author(s) 2026. CC BY 4.0 License.

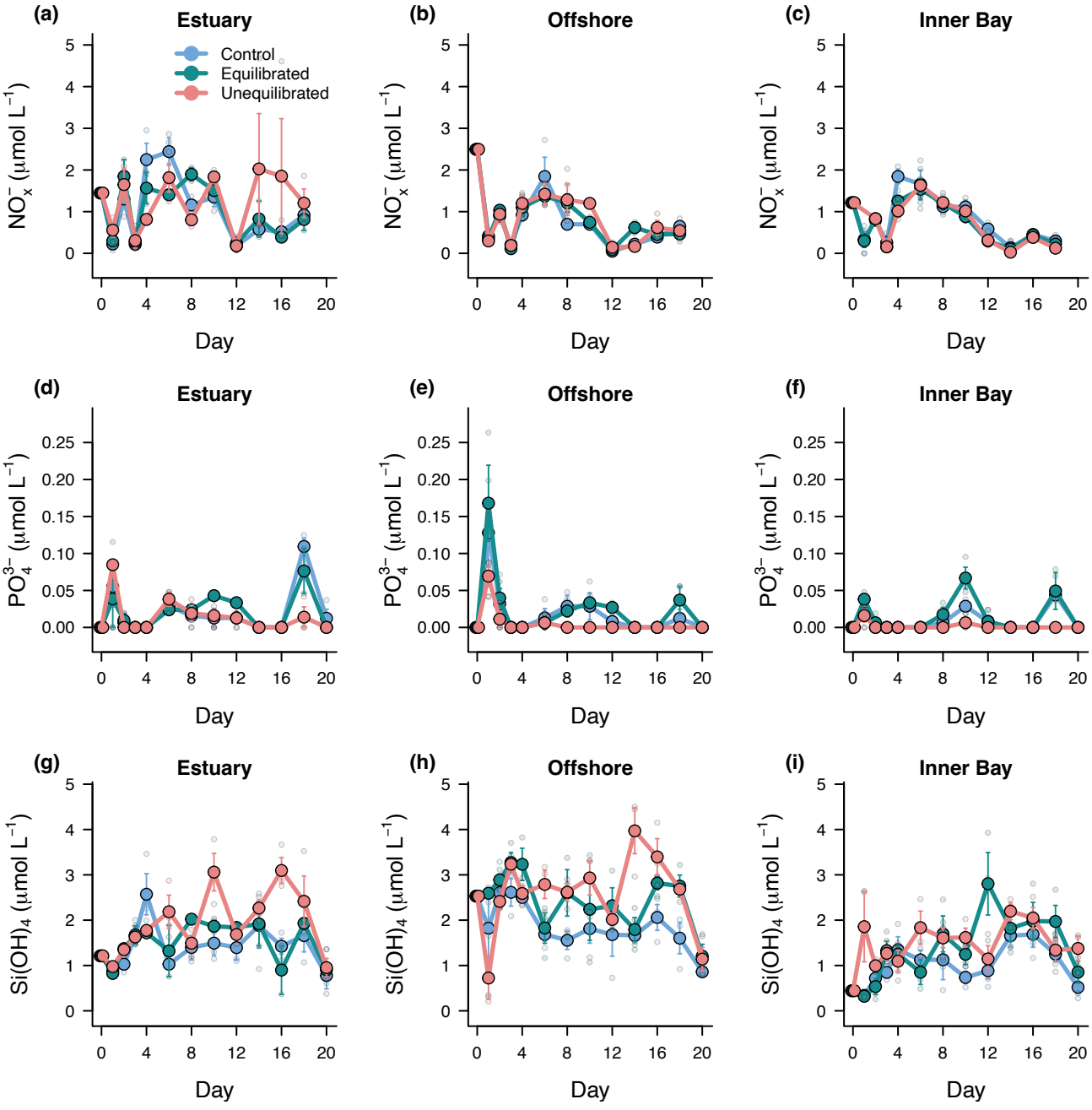


Figure 3. Temporal changes in dissolved nutrients across the three source-water experiments. Panels show nitrate plus nitrite (NO_x^-; a–c), phosphate (PO_4^{3-}; d–f), and dissolved silicic acid ($Si(OH)_4$; g–i). Columns represent Estuary, Offshore, and Inner Bay, respectively. Small translucent points represent individual biologically independent microcosms, whereas coloured circles and solid lines show observed arithmetic treatment means. Error bars indicate ±1 standard error where at least two replicates were available; some are smaller than the symbols. Each treatment comprised up to three biological replicates per sampling day. NO_x^- measurements were unavailable on Day 20.

https://doi.org/10.5194/egusphere-2026-6827
Preprint. Discussion started: 19 November 2026
© Author(s) 2026. CC BY 4.0 License.

Chlorophyll-a showed a strong temporal decline across all three source-water types, with no consistent separation among OAE exposure scenarios (Figure 4). Initial mean chlorophyll-a concentrations were highest in the Offshore experiment (33.6–51.7 μg L^{-1}) and lower in the Estuary and Inner Bay experiments (17.4–21.9 μg L^{-1}). Across all source waters, chlorophyll-a declined rapidly during the first 2–4 days and then remained comparatively low for the remainder of the incubation. This shared temporal pattern dominated over the relatively small and source-water-dependent treatment differences. GAMM contrasts provided no evidence for a sustained difference between the equilibrated and unequilibrated treatments across the three source-water types. Similar temporal declines in chlorophyll-a and phytoplankton biomass are commonly observed during incubations in Daya Bay (Liu et al., 2012, 2026; Song et al., 2004; Sun et al., 2011).

Treatment differences were consistently small and varied among source waters. In the Estuary experiment, the two OAE treatments followed similar low-biomass trajectories after the initial decline (Figure 4a). In the Offshore experiment, the large initial biomass declined sharply in all treatments, and neither OAE treatment produced a persistent biomass increase relative to the other treatment or the control (Figure 4b). In the Inner Bay experiment, chlorophyll-a was slightly higher in the control and equilibrated treatments than in the unequilibrated treatment toward the end of the incubation (Figure 4c), but this pattern was not repeated in the Estuary or Offshore experiments. Thus, the strong carbonate-chemistry contrast was not associated with a consistent chlorophyll-a response across source waters.

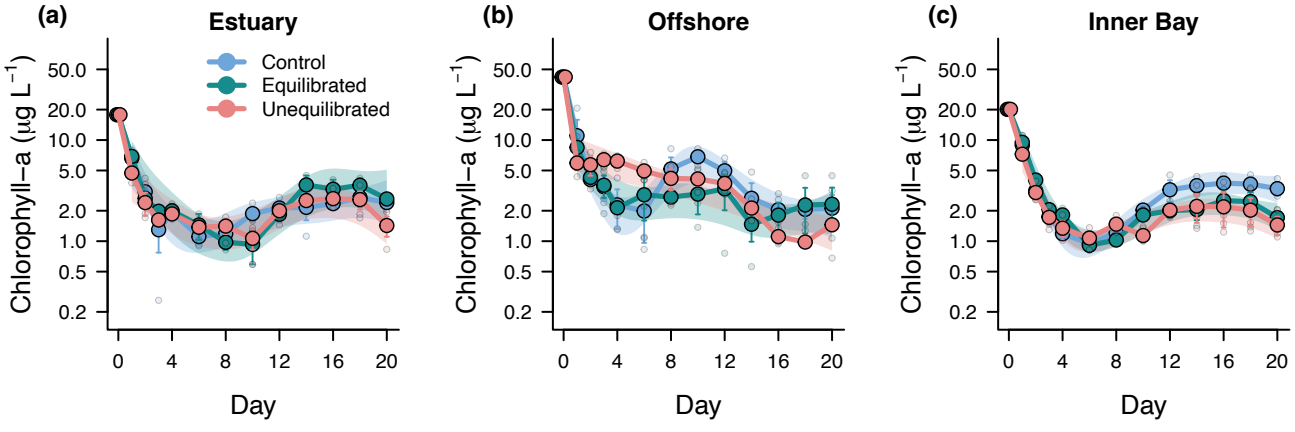


Figure 4. Temporal changes in chlorophyll-a across the three source-water experiments. Columns represent Estuary, Offshore, and Inner Bay, respectively. Small translucent points represent individual biologically independent microcosms, whereas coloured circles and solid lines show observed arithmetic treatment means. Error bars indicate ±1 standard error where at least two replicates were available; some are smaller than the symbols. Each treatment comprised up to three biological replicates per sampling day. Chlorophyll-a is plotted on a logarithmic y-axis. Coloured ribbons in panels (a–c) show 95% pointwise confidence intervals for population-level geometric mean trajectories estimated using generalised additive mixed models (GAMMs). Day 0 represents pre-addition conditions and was excluded from GAMM fitting, which used observations from Days 1–20.

https://doi.org/10.5194/egusphere-2026-6827
Preprint. Discussion started: 19 November 2026
© Author(s) 2026. CC BY 4.0 License.

Flow cytometry resolved temporal trajectories of distinct operationally defined groups that were not captured by bulk chlorophyll-a alone (Figure 5). The picophytoplankton (Pico), *Synechococcus* (Syn), and nanophytoplankton (Nano) populations all showed substantial variation among source waters and through the incubation. The Day 0 baseline provides an initial reference value for each water mass prior to any treatments being added. Subsequent trajectories differed among Estuary, Offshore, and Inner Bay communities, and treatment lines did not show a uniform ordering of equilibrated and unequilibrated exposures across all three population classes. The strongest contrasts were therefore conditional on source-water context and sampling day rather than being shared responses to one OAE scenario.

No uniform separation between the equilibrated and unequilibrated treatments was observed across the three population groups and source waters. These data therefore indicate that flow-cytometric responses were conditional on source-water context and sampling day, with no consistent treatment-specific pattern across the experiments. This is consistent with previous experiments from the same region in 55 L and 50,000 L scale experiments using $Mg(OH)_2$ as an alkalinity source, but with lower TA additions (Liu et al., 2026).

Chloroplast-associated profiles showed treatment differences that were not apparent in bulk chlorophyll-a or the prokaryotic community (Figure 6). In Estuary and Inner Bay source waters, the relative abundance of Unclassified Gyrista increased in the unequilibrated treatment, while Mamiellophyceae decreased. In the Inner Bay equilibrated treatment, Dictyochophyceae also tended to increase, although the direction was inconsistent among biological replicates. Across all treatments, incubation and source water remained strong determinants of the background phytoplankton signal: Mediophyceae were prominent in Day 0 Offshore samples, whereas Mamiellophyceae became dominant in many Day 20 communities. The treatment-associated patterns are therefore best interpreted as taxon-specific and conditional responses superimposed on strong temporal succession patterns.

The 18S profiles partly overlapped with the chloroplast signal but did not reproduce it uniformly (Figure S3). Mamiellophyceae had lower relative abundance in unequilibrated communities, whereas Bacillariophyceae was higher in the Inner Bay unequilibrated treatment than in the control and equilibrated treatments. Dinophyceae declined through incubation across source waters. The correspondence between higher Bacillariophyceae and Unclassified_Gyrista:plas in the Inner Bay is consistent with, but on its own does not establish, a diatom contribution to the chloroplast signal. The low rarefied depth (408 reads) further limits detection of less abundant taxa; these data therefore provide exploratory relative-abundance evidence rather than evidence of biomass change, survival advantage or a carbon-concentrating mechanism.

https://doi.org/10.5194/egusphere-2026-6827
Preprint. Discussion started: 19 November 2026
© Author(s) 2026. CC BY 4.0 License.

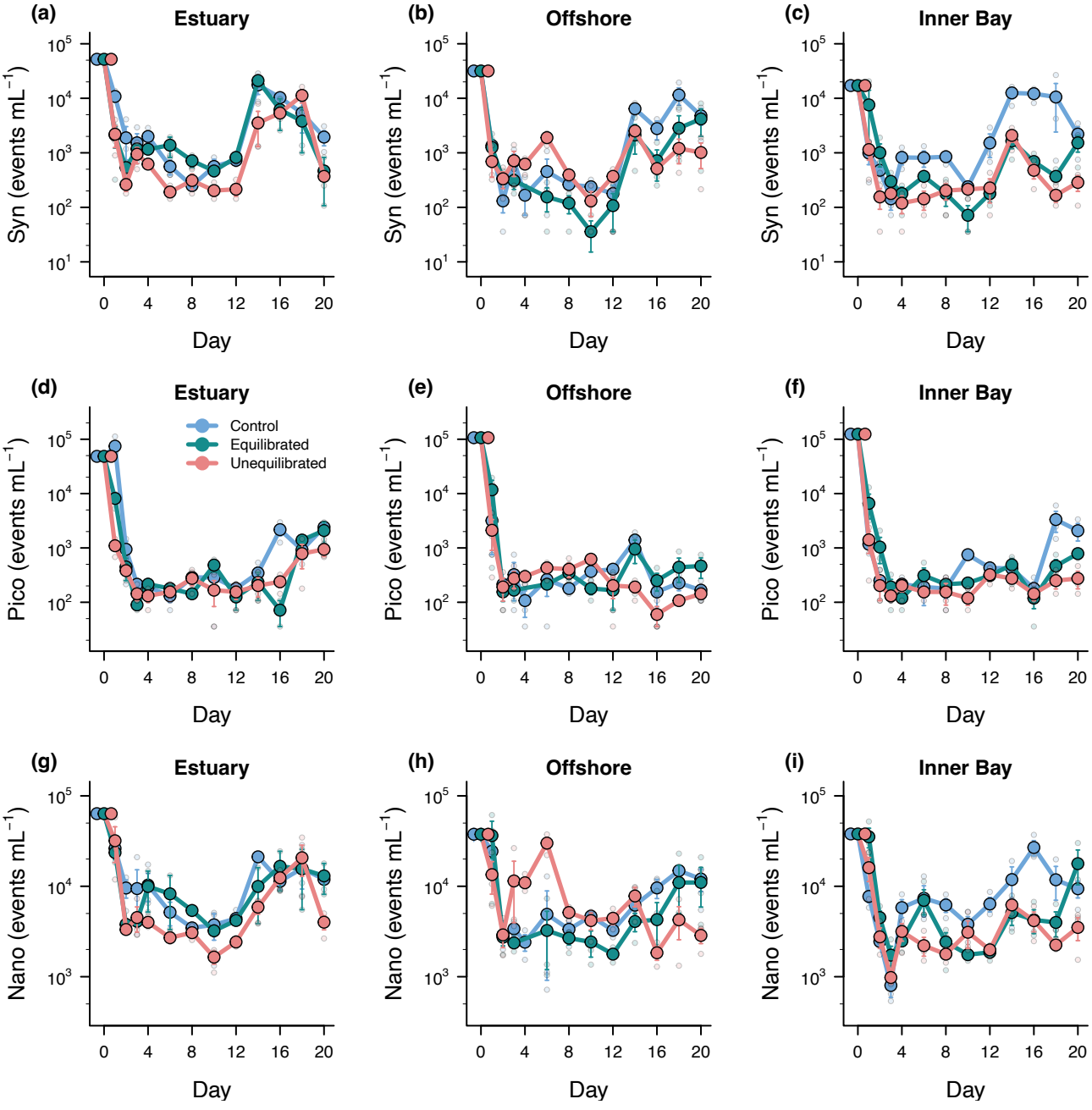


Figure 5. Flow-cytometry derived plankton population trends. Panels show (a-c) Synechococcus (Syn), (d-f) picophytoplankton (Pico), and (g-i) nanophytoplankton (Nano) populations for Estuary, Offshore, and Inner Bay source waters under control, CO_2-equilibrated OAE, and CO_2-unequilibrated OAE treatments. Points and lines show treatment means and error bars show standard errors among biological replicates. Day 0 represents a common baseline for each source-water type; subsequent values are calculated from sample-level calibrated counts.

https://doi.org/10.5194/egusphere-2026-6827
Preprint. Discussion started: 19 November 2026
© Author(s) 2026. CC BY 4.0 License.

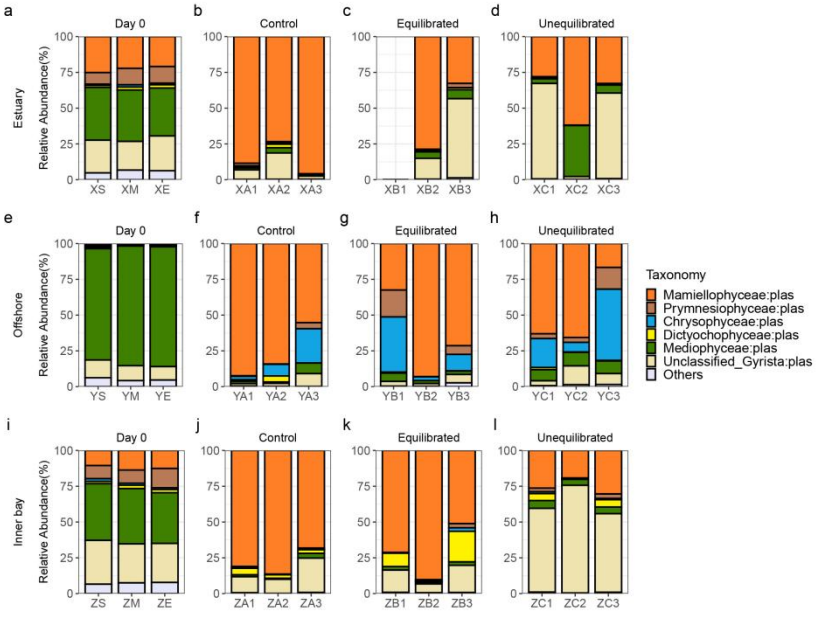


Figure 6. Phytoplankton community structure based on chloroplast sequences re-annotated with PR2. Relative abundances are shown at class level for the three source waters and the control, equilibrated and unequilibrated treatments. The ":plas" suffix denotes plastid-associated (chloroplast) annotations. XB1, without data, refers to the incubator which was withdrawn from the experiment after day 1 due to a faulty aquarium heater.

3.3 Microbial community profiles showed modest, source-water-dependent taxon responses

Whilst flow cytometry provided an overview of temporal changes in size fractionated microbial groups, further detail was provided by rRNA-gene amplicon sequencing. 16S rRNA gene amplicon sequencing also showed that prokaryotic communities were structured primarily by incubation time and source-water context, rather than by OAE exposure scenario (Figure 7). Across source waters and treatments, communities were dominated by Alphaproteobacteria, especially SAR11-related lineages, with Bacteroidota and Gammaproteobacteria also contributing substantially (Figure S1). Contrasting the start and end of the incubations, there was a broad shift in community composition: HIMB11 and unclassified Rhodobacteraceae generally declined, whereas the AEGEAN-169 marine group and Cyanobacteria generally increased (Figure S2). Alpha diversity, estimated using Simpson's index, was generally lower at the end of the incubation than in the initial source-water samples. NMDS ordination showed a clear separation between initial and final communities (ANOSIM R = 0.670, *p*-value = 0.001), with a weaker source-water signal, particularly for Offshore samples. In contrast, final communities from equilibrated and unequilibrated treatments did not form a consistent separation across all source waters. Predicted functional profiles showed the same qualitative pattern: individual functions varied among source waters and through the incubation, but did not show persistent ordering corresponding to the two OAE exposure scenarios (Table. S1). These microbial data therefore support the conclusion that community responses did not track the imposed carbonate-chemistry contrast between exposure scenarios.

https://doi.org/10.5194/egusphere-2026-6827
Preprint. Discussion started: 19 November 2026
© Author(s) 2026. CC BY 4.0 License.

This is consistent with prior analysis of prokaryotic community responses to OAE in Daya Bay using $Mg(OH)_2$ at lower doses (Liu et al., 2026).

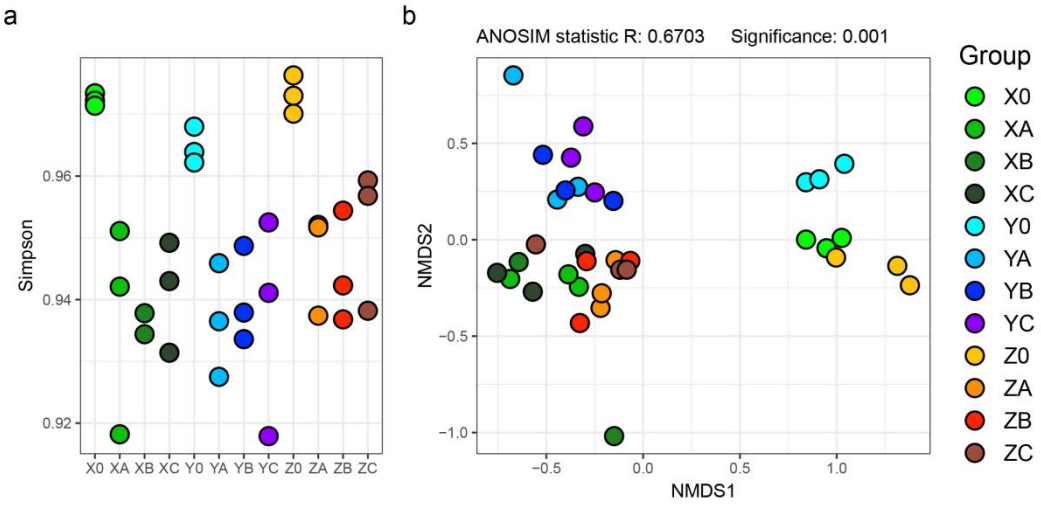


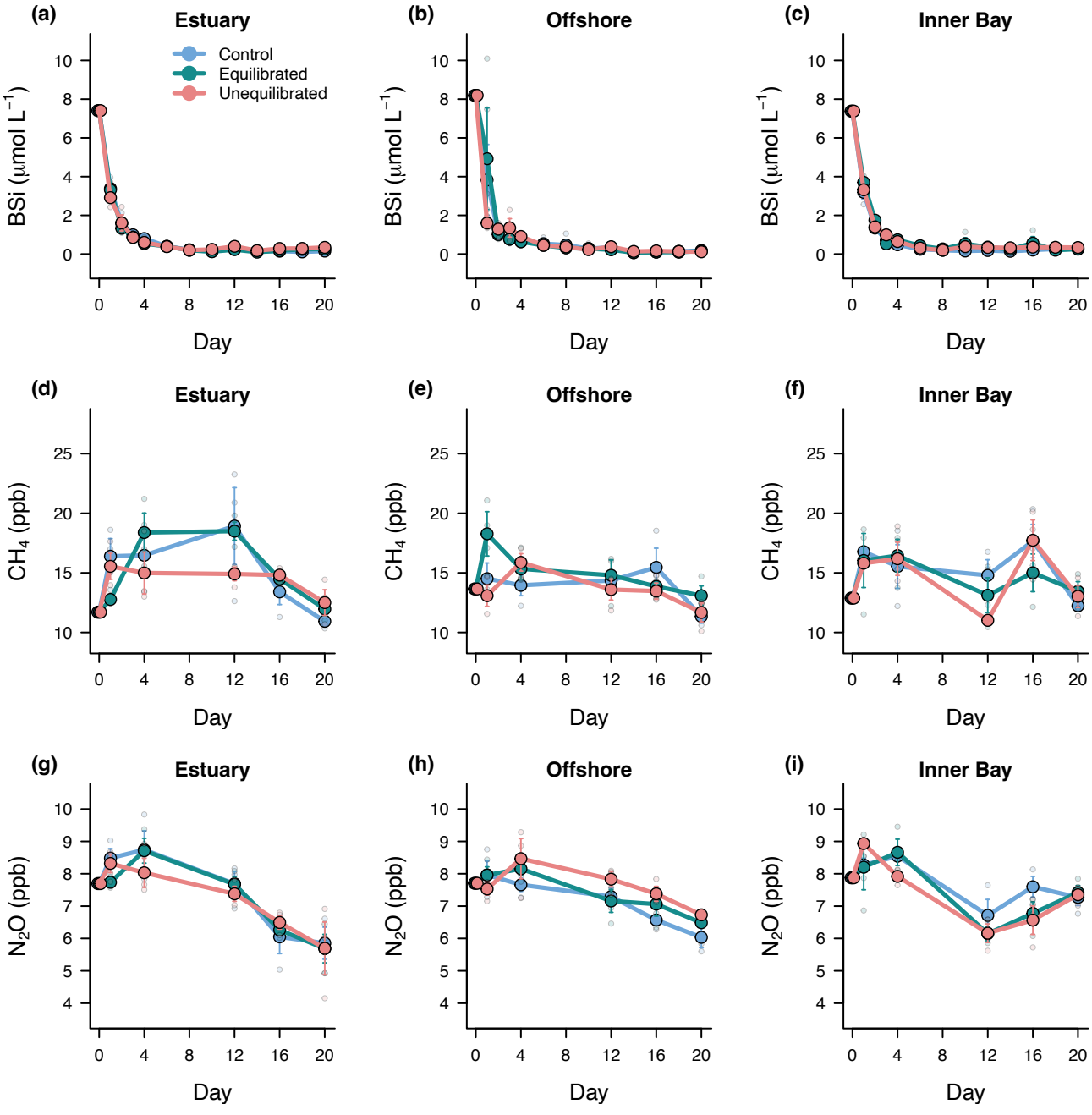
Figure 7. Alpha- and beta-diversity patterns of prokaryotic communities based on 16S rRNA gene amplicon sequencing. Panel (a) shows Simpson diversity. Panel (b) shows non-metric multidimensional scaling (NMDS) of prokaryotic community composition. ANOSIM indicates an overall separation among sample groups (R = 0.6703, *p*-value = 0.001), driven mainly by the initial-versus-final contrast rather than a common treatment separation. Group labels are X = Estuary, Y = Offshore, Z = Inner Bay; A = Control, B = CO_2-equilibrated OAE, and C = CO_2-unequilibrated OAE. 'X0', 'Y0' and 'Z0', without a treatment designation, are the initial conditions.

3.4 Other dissolved greenhouse gases showed episodic variability without a shared OAE trajectory

Biogenic silica also declined rapidly during the first few days in all three source waters, broadly tracking the early decline in chlorophyll-a (Figure 8a–c). Initial mean BSi was highest in the Offshore experiment (7.8–8.5 μmol L^{-1}) and was slightly lower in the Estuary and Inner Bay experiments (6.5–8.0 μmol L^{-1}). After day 4, BSi generally remained below 1 μmol L^{-1} in most treatments. The BSi data therefore indicated a rapid decline in silica-rich suspended biomass during the early incubation, but provided limited evidence for a consistent silica-related response to the equilibrated versus unequilibrated OAE scenario. Notably, as BSi declined there was no corresponding increase in $Si(OH)_4$, indicating that most BSi was lost via aggregation and/or settling without dissolution to form $Si(OH)_4$.

Dissolved CH_4 and N_2O concentrations showed short-lived, source-water-dependent treatment differences (Figure 8d–i). However, these differences were not repeated across source waters or maintained through time. They therefore indicate modest transient temporal variation rather than a common response to the imposed OAE treatments. Of the two main greenhouse gases after CO_2, N_2O formation is likely to be more sensitive to OAE following NaOH addition as pH gradients in estuaries are often shown to affect, or at least correlate with, N_2O formation rates (Amaral et al., 2021; Zhou et al., 2024). Yet no consistent treatment-associated pattern was observed for either CH_4 or N_2O across the three source waters.

https://doi.org/10.5194/egusphere-2026-6827
Preprint. Discussion started: 19 November 2026
© Author(s) 2026. CC BY 4.0 License.



385 **Figure 8. Temporal changes in biogenic silica and dissolved greenhouse gases (CH_4 and N_2O). (a-c) biogenic silica (BSi), (d-f) CH_4, (g-h)N_2O for Estuary, Offshore, and Inner Bay source waters. Points indicate individual biologically independent microcosms, lines show treatment means, and error bars show standard errors where at least two replicate measurements were available. Gas measurements were made on Days 0, 1, 4, 12, 16, and 20. Concentrations are reported in ppb.**

https://doi.org/10.5194/egusphere-2026-6827
Preprint. Discussion started: 19 November 2026
© Author(s) 2026. CC BY 4.0 License.

4 Discussion

4.1 Contrasting carbonate chemistry trajectories and apparent alkalinity loss

The equilibrated and unequilibrated treatments created different carbonate chemistry exposures in all three Daya Bay source waters. This is the contrast that OAEPIIP was designed to test: the unequilibrated treatment represents the high pH state occurring soon after NaOH addition, whereas the equilibrated treatment represents a conceptually later state in which added alkalinity is accompanied by additional DIC after CO_2 exchange (Bach et al., 2024; Schulz et al., 2023).

The equilibrated treatment remained close to the intended +500 µmol kg^{-1} TA increase. The unequilibrated treatment retained only part of this increase. Differences between added and measured alkalinity could arise for several reasons (Hartmann et al., 2023; He and Tyka, 2022; Ringham et al., 2024). Insufficient mixing early in the experiment can be excluded as a potential driver of the observed trend as this would also have affected the equilibrated additions, and the observed TA trends were highly reproducible between replicates. The loss was also immediately apparent within the first measurements after NaOH addition and thus cannot be primarily attributed to biogenic calcification. The most plausible explanation for apparent TA loss is therefore spontaneous secondary carbonate precipitation.

Secondary carbonate precipitation was not anticipated as a possible TA sink in the OAEPIIP design because the TA doses applied are relatively low, and the use of NaOH -rather than an alkaline mineral- reduces the risk of heterogeneous calcium carbonate precipitation on mineral surfaces (Suitner et al., 2024, 2026). Nevertheless, coastal regions with higher particle loads compared to offshore pelagic environments, are susceptible to heterogeneous calcium carbonate precipitation at relatively low calcium carbonate saturation states (Tian et al., 2025).

We calculated the aragonite saturation state Ω_{arag} from measured TA, DIC, temperature and salinity in CO_2SYS. On Day 1, mean Ω_{arag} across the three source waters was 2.91 in the control, 4.34 in the equilibrated treatment and 5.75 in the unequilibrated treatment (Figure S4). During Days 1–4, when source-water mean Ω_{arag} in the unequilibrated treatment reached its maxima, Ω_{arag} averaged 2.85, 4.18 and 5.86 in the control, CO_2-equilibrated and CO_2-unequilibrated treatments, respectively, across sampling days and source waters. Peak mean values in the unequilibrated treatment were 5.92 in Inner Bay on Day 1, 5.68 in the Estuary on day 4, and 6.42 in the Offshore water on Day 4. Thus, all treatments were supersaturated, but the early unequilibrated treatment, as would be expected, had the highest saturation states and the greatest potential for secondary carbonate precipitation. Several studies have suggested higher thresholds are required for the triggering of this process. Aragonite precipitation is, for example, observed above 7 Ω_{arag} in the presence of $Ca(OH)_2$ (Moras et al., 2022). The specific trigger for secondary carbonate precipitation is nucleation, as this process maintains the kinetic barrier to spontaneous $CaCO_3$ formation under supersaturated conditions (Sun et al., 2015). Thus, whilst conditions <5 Ω_{arag} are often considered to be a 'safe' limit to avoid secondary carbonate precipitation in seawater, this is not strictly valid in particle-rich water as diverse nucleating agents can trigger aragonite precipitation at lower saturation thresholds (Stanton et al., 2023; Wurgaft et al., 2021). This has

https://doi.org/10.5194/egusphere-2026-6827
Preprint. Discussion started: 19 November 2026
© Author(s) 2026. CC BY 4.0 License.

been demonstrated in estuarine environments and a similar mechanism is likely behind 'whiting events' in the Caribbean occur at conditions <5 Ω_{arag} (Long et al., 2017; Wurgaft et al., 2021).

In closed incubations, constraining the extent of any calcium carbonate precipitation is relatively straightforward as any formation of $CaCO_3$ proceeds with a characteristic 2:1 decline in TA:DIC (Hartmann et al., 2023; Moras et al., 2022; Suitner et al., 2024). However, in open systems with air-sea CO_2 exchange, and biota as a major driver of changing DIC dynamics, this ratio is often masked by other processes. The OAEPIIP experiment design is not therefore well designed to investigate the TA loss mechanism at play. However, it clearly warrants further investigation in coastal environments which are of interest for OAE trials due primarily to reduced costs.

Whilst NaOH is often preferred as an alkalinity source because it does not provide a surface area that can trigger secondary carbonate precipitation, this is also not strictly correct. NaOH addition to seawater does often generate a precipitate which is thought to be largely $Mg(OH)_2$ and to be re-dissolved rapidly (Kapp, 1928). The OAEPIIP includes a mixing task after NaOH addition exactly for this reason (Bach et al., 2024). We can speculate that if $Mg(OH)_2$, or other precipitates, do not fully and rapidly re-dissolve they may be key triggers for secondary carbonate precipitation following NaOH addition to seawater. There are however also many other plausible triggers for nucleation in unfiltered coastal seawater. For example, in addition to lithogenic mineral particles, some diatoms are thought to act as nucleating agents under some conditions, which might be of significance given the strong diatom bloom that was underway at the start of all three experiments herein (Chen et al., 2025a; Ouyang et al., 2018; Pan et al., 2024; Tesson et al., 2008).

Whilst the present data cannot further elaborate on the exact cause of TA loss herein, it should be noted that apparent TA loss is also reported elsewhere in other OAE work regionally. Another OAEPIIP experiment in a similar locality under summertime conditions noted a similar phenomenon (Xin et al., 2026). In this case, high temperature was speculated to have facilitated a lower threshold for secondary carbonate precipitation. Yet herein, temperatures averaged 17°C and never exceeded 19°C which is relatively low in the geographic location and close to the annual minima. Similarly, OAE trials with $Mg(OH)_2$ in Daya Bay at lower doses than used herein reported an apparent inefficiency with the underlying cause undetermined (Liu et al., 2026). A precise Ca and Mg mass balance (Bach et al., 2026; Ho et al., 2023; Schulz et al., 2023), or more detailed spectroscopy of the particles formed during the experiments would be necessary to further interpret the TA dynamics.

4.2 Limited and context-dependent biological responses

Throughout all experiments herein, the gradients imposed in carbonate chemistry were not matched by clear responses in most biological parameters. Apparent TA loss in the unequilibrated treatment reduced the retained alkalinity enhancement below the nominal +500 µmol kg^{-1} addition and thus the unequilibrated and equilibrated treatments are less directly comparable than was envisaged in the OAEPIIP design. Ecological responses should therefore be interpreted in relation to the measured carbonate chemistry trajectories, accounting for both alkalinity retention and CO_2 equilibration (Bach et al., 2024; Schulz et al., 2023).

https://doi.org/10.5194/egusphere-2026-6827
Preprint. Discussion started: 19 November 2026
© Author(s) 2026. CC BY 4.0 License.

Temporal trajectories of chlorophyll-a, flow-cytometric groups, nutrients, BSi and prokaryotic communities were all unremarkable and failed to show clear evidence of differences between treatments. The three experiments conducted herein were all initiated on the same day using source water from three localities within the same bay. The strong differences between source waters are therefore indicative of the spatial-temporal variability naturally present in this coastal environment, where water is resident for time periods of a few weeks to a month (Zhang et al., 2019). The dominance of source-water differences over treatment-associated patterns is consistent with any biogeochemical or ecological responses being smaller than the background variability resolved here. This is an important insight for Monitoring, Reporting and Verification of any potential ecological side-effects of OAE trials (Ho et al., 2023). In this regional environmental context, any monitoring of open water OAE trials at lower doses would be unable to detect shifts attributable to alkalinity addition as background variability is larger. The same conclusion was reached in prior work in Daya Bay by comparing the temporal evolution of ecological conditions during enclosed OAE trials with background variability in the adjacent bay area (Liu et al., 2026). This notion justifies investment in large-scale enclosed experiments as these are one of the only ways insights into any side-effects of OAE can be investigated under environmentally relevant conditions without being masked by environmental variability. Variable effects among coastal plankton communities, together with weak short term stress in an open ocean community, have been reported in other OAE experiments (Ferderer et al., 2022; Guo et al., 2024; Paul et al., 2025; Ramírez et al., 2025).

The initial community state may also have influenced the ecological responses (Subhas et al., 2022). The shared early decline in chlorophyll-a and BSi across three experiments herein was consistent with the waning of a diatom bloom. Low initial nutrient concentrations may have constrained growth responses to the carbonate chemistry perturbation, although nutrient limitation was not directly tested. The limited treatment-associated responses should therefore be interpreted within this seasonal and community context, with responses during other bloom stages remaining unresolved (Sun et al., 2011). Whilst the core biogeochemical and ecological parameters showed no clear evidence of OAE treatment effects, the chloroplast and 18S data suggested that bulk measurements may hide taxon specific responses. The changes in Mamiellophyceae, Bacillariophyceae and Gyrista were consistent with a source water dependent response to the high pH and low pCO_2 trajectory induced by unequilibrated alkalinity addition. Elsewhere, taxon specific gains and losses have been reported under hydroxide based OAE (Kousoulas et al., 2025). Whilst these data do not identify a physiological mechanism, we note that even the strongest pH and pCO_2 changes induced by OAE herein did not exceed the range of naturally observed conditions within Daya Bay (Chen et al., 2024; Wang et al., 2022). It is therefore debatable if subtle, taxon specific effects justify more specific targeted physiological measurements to understand the specific mechanistic relationships at play in the context of critically evaluating OAE.

Whilst OAE directly affects CO_2 dynamics, a key question with any proposed carbon sequestration technology is whether or not it affects other greenhouse gas dynamics. Unfortunately, several proposed climate interventions with positive effects on carbon storage likely suffer some degree of offsets due to increased CH_4 and N_2O formation. Throughout all three experiments, there was no clear effect of OAE treatments on CH_4 and N_2O. Whilst measured concentrations alone cannot distinguish

https://doi.org/10.5194/egusphere-2026-6827
Preprint. Discussion started: 19 November 2026
© Author(s) 2026. CC BY 4.0 License.

production or consumption of these dissolved components, this suggests that there was no detectable effect of OAE on overall CH_4 and N_2O dynamics under the conditions tested. The main hypothesized effect is that pH may affect N_2O formation, which is evident in many estuarine studies (Amaral et al., 2021; Zhou et al., 2024). However, the pH change herein was modest potentially explaining why no significant effect was evident.

4.3 Implications for OAE assessment and experimental limitations

The experiments herein allow the clear separation of chemical sensitivity from ecological sensitivity. Whilst the conclusions are limited to the Daya Bay source waters, the trio of experiments demonstrate the reproducible loss of alkalinity in a nearshore system and limited evidence of biogeochemical or ecological responses to both equilibrated and unequilibrated OAE over a short (20 day) experimental timeframe.

Whilst 55 L is a sufficiently large volume to facilitate a good degree of chemical and ecological reproducibility between treatments, bottle conditions cannot resolve the more realistic OAE scenario where an initial pulse of increased alkalinity is rapidly diluted. Similarly, the OAEPIIP setup is not informative concerning benthic-pelagic coupling, which is particularly important in shallow, coastal environments such as the largely <10 m depth bay used as a field site herein. Nevertheless, short incubations are valuable for identifying exposure and response pathways, even if they cannot by themselves predict field persistence or carbon removal durability (Ho et al., 2023; Riebesell et al., 2023). The replicated design of the OAEPIIP trial is also critical for eliminating the possibility of unforeseen or dubious methodological issues from individual experiments.

5 Conclusions

A trio of 55 L incubation experiments was conducted in Daya Bay assessing the effects of unequilibrated and equilibrated NaOH addition to seawater over 20-day incubations. The unequilibrated and equilibrated NaOH additions followed different trajectories. In all three cases, equilibrated NaOH produced a TA change within uncertainty of the calculated addition with a corresponding increase in DIC. Yet unequilibrated NaOH additions did not reach the calculated TA addition indicating a TA loss process. The underlying mechanism of this TA loss cannot be verified from data herein, but was likely heterogeneous secondary carbonate precipitation.

The induced carbonate chemistry responses to OAE did not drive consistent, treatment-specific responses in bulk biomass, macronutrients, greenhouse gases (N_2O and CH_4) or prokaryotic communities. Chloroplast and 18S profiles instead suggested modest, taxon-specific treatment differences that varied among source waters. Whilst the 20-day incubations conducted here are insufficient to prove that long term OAE treatments are benign, the doses (+500 µmol kg^{-1}) applied were also likely higher than what would be experienced, even temporarily, during a sustained open water OAE trial. The absence of biogeochemical or ecological responses, relative to strong spatial changes within the bay area, further indicates that natural spatial and temporal variability would likely mask any associated effects at the lower doses of any open water OAE trial in a similar region.

https://doi.org/10.5194/egusphere-2026-6827
Preprint. Discussion started: 19 November 2026
© Author(s) 2026. CC BY 4.0 License.

Data availability

The experimental data have been shared with Dr Lennart Bach (lennart.bach@utas.edu.au), the OAEPIIP coordinator, to produce a coordinated global OAEPIIP database. Data have also been deposited at Figshare (https://doi.org/10.6084/m9.figshare.34831815). The raw sequencing data are available at National Center for Biotechnology Information (PRJNA1550244).

Author contributions

XW and MH conceptualized the study and prepared the original draft. YL, APV, RB, RN, QJ and SH contributed to methodology, investigation, analysis, and manuscript revision. All authors reviewed and edited the manuscript.

Competing interests

The authors declare that they have no conflict of interest.

Acknowledgements

We thank the OAEPIIP team for assistance with field sampling, laboratory analyses, and project coordination. We also thank Professor Qiang Zheng and Dr Bowen He from Xiamen University for their assistance with flow cytometry measurements.

Financial support

This work was supported by grants from the Science Fund Program for Distinguished Young Scholars (Overseas) of Mark James Hopwood (Reference number: 4211101149), the National Natural Science Foundation of China (42476109, 42276163 and 42550048 to S.H.), the Shenzhen Science and Technology Innovation Bureau Key R&D Program (ZDCYKCX20250901092703004 to S.H.), the Guangdong Outstanding Young Talent Program (2023QN10H604 to S.H.), the SUSTech Education Reform Program (SJZLGC202437 to S.H.), and the OAEPIIP project coordinated by the University of Tasmania.

References

Amaral, V., Ortega, T., Romera-Castillo, C., and Forja, J.: Linkages between greenhouse gases (CO_2, CH_4, and N_2O) and dissolved organic matter composition in a shallow estuary, Science of The Total Environment, 788, 147863, https://doi.org/10.1016/j.scitotenv.2021.147863, 2021.

https://doi.org/10.5194/egusphere-2026-6827
Preprint. Discussion started: 19 November 2026
© Author(s) 2026. CC BY 4.0 License.

Bach, L. T.: The additionality problem of ocean alkalinity enhancement, Biogeosciences, 21, 261–277, https://doi.org/10.5194/bg-21-261-2024, 2024.

Bach, L. T., Gill, S. J., Rickaby, R. E. M., Gore, S., and Renforth, P.: CO_2 Removal With Enhanced Weathering and Ocean Alkalinity Enhancement: Potential Risks and Co-benefits for Marine Pelagic Ecosystems, Front. Clim., 1, 7, https://doi.org/10.3389/fclim.2019.00007, 2019.

Bach, L. T., Ferderer, A. J., LaRoche, J., and Schulz, K. G.: Technical note: Ocean Alkalinity Enhancement Pelagic Impact Intercomparison Project (OAEPIIP), Biogeosciences, 21, 3665–3676, https://doi.org/10.5194/bg-21-3665-2024, 2024.

Bach, L. T., Atamanchuk, D., Britton, D., Fuhr, M., Hylén, A., Nawaz, S., and Rohr, T.: Rethinking ocean alkalinity enhancement, Nat Rev Earth Environ, 7, 725–742, https://doi.org/10.1038/s43017-026-00828-5, 2026.

Bolyen, E., Rideout, J. R., Dillon, M. R., Bokulich, N. A., Abnet, C. C., Al-Ghalith, G. A., Alexander, H., Alm, E. J., Arumugam, M., and Asnicar, F.: Reproducible, interactive, scalable and extensible microbiome data science using QIIME 2, Nature biotechnology, 37, 852–857, https://doi.org/10.1038/s41587-019-0209-9, 2019.

Boyd, P., Collins, S., Dupont, S., Fabricius, K., Gattuso, J.-P., Havenhand, J., Hutchins, D. A., McGraw, C. M., Riebesell, U., and Vichi, M.: SCOR WG149 Handbook to support the SCOR Best Practice Guide for'Multiple Drivers ‚Äö'Marine Research, https://doi.org/10.25959/5c92fdf0d3c7a, 2019.

Callahan, B. J., McMurdie, P. J., Rosen, M. J., Han, A. W., Johnson, A. J. A., and Holmes, S. P.: DADA2: High-resolution sample inference from Illumina amplicon data, Nature methods, 13, 581–583, https://doi.org/10.1016/j.marchem.2025.104533, 2016.

Chen, Q., Li, Y., Chen, C.-T. A., Jiang, Z.-P., Cai, W.-J., Pan, H., Shen, Y., Ding, Z., Di, Y., Zhu, C., Jiao, N., and Pan, Y.: Diatom-induced calcification in coastal marine environments: Biomineralization threshold and mechanism, Marine Chemistry, 271, 104533, https://doi.org/10.1016/j.marchem.2025.104533, 2025a.

Chen, S., Arifeen, M. Z. U., Li, M., Xu, S., Wang, H., Chen, S., Tao, J., Guo, K., Yan, R., Zheng, Y., Hou, S., and Zhang, C.: Diel Patterns in the Composition and Activity of Planktonic Microbes in a Subtropical Bay, Ocean-Land-Atmosphere Research, 3, 0044, https://doi.org/10.34133/olar.0044, 2024.

Chen, Z., Yu, L., Yang, Q., and Ji, Q.: Discerning natural and anthropogenic factors driving the variation of estuarine CH_4 and N_2O, Ocean-Land-Atmosphere Research, 4, 0080, https://doi.org/10.34133/olar.0080, 2025b.

DeMaster, D. J.: The supply and accumulation of silica in the marine environment, Geochimica et Cosmochimica acta, 45, 1715–1732, https://doi.org/10.1016/0016-7037(81)90006-5, 1981.

Dickson, A. G.: Standard potential of the reaction: AgCl (s)+ 12H_2 (g)= Ag (s)+ HCl (aq), and and the standard acidity constant of the ion HSO_4^- in synthetic sea water from 273.15 to 318.15 K, The Journal of Chemical Thermodynamics, 22, 113–127, https://doi.org/10.1016/0021-9614(90)90074-Z, 1990.

Eisaman, M. D., Geilert, S., Renforth, P., Bastianini, L., Campbell, J., Dale, A. W., Foteinis, S., Grasse, P., Hawrot, O., Löscher, C. R., Rau, G. H., and Rønning, J.: Assessing the technical aspects of ocean-alkalinity-enhancement approaches, State of the Planet, 2-oae2023, 1–29, https://doi.org/10.5194/sp-2-oae2023-3-2023, 2023.

https://doi.org/10.5194/egusphere-2026-6827
Preprint. Discussion started: 19 November 2026
© Author(s) 2026. CC BY 4.0 License.

Ferderer, A., Chase, Z., Kennedy, F., Schulz, K. G., and Bach, L. T.: Assessing the influence of ocean alkalinity enhancement on a coastal phytoplankton community, Biogeosciences, 19, 5375–5399, https://doi.org/10.5194/bg-19-5375-2022, 2022.

Frey, C., Tang, W., Ward, B. B., and Lehmann, M. F.: Sample preservation methods for nitrous oxide concentration and isotope ratio measurements in aquatic environments, Limnology and Oceanography: Methods, 22, 771–788, https://doi.org/10.1002/lom3.10638, 2024.

Gattuso, J.-P., Williamson, P., Duarte, C. M., and Magnan, A. K.: The Potential for Ocean-Based Climate Action: Negative Emissions Technologies and Beyond, Front. Clim., 2, https://doi.org/10.3389/fclim.2020.575716, 2021.

Goreau, T. J., Kaplan, W. A., Wofsy, S. C., McElroy, M. B., Valois, F. W., and Watson, S. W.: Production of NO_2^- and N_2O by nitrifying bacteria at reduced concentrations of oxygen, Applied and environmental microbiology, 40, 526–532, https://doi.org/10.1128/aem.40.3.526-532.1980, 1980.

Guillou, L., Bachar, D., Audic, S., Bass, D., Berney, C., Bittner, L., Boutte, C., Burgaud, G., De Vargas, C., and Decelle, J.: The Protist Ribosomal Reference database (PR2): a catalog of unicellular eukaryote small sub-unit rRNA sequences with curated taxonomy, Nucleic acids research, 41, D597–D604, https://doi.org/10.1093/nar/gks1160, 2012.

Guo, J. A., Strzepek, R. F., Swadling, K. M., Townsend, A. T., and Bach, L. T.: Influence of ocean alkalinity enhancement with olivine or steel slag on a coastal plankton community in Tasmania, Biogeosciences, 21, 2335–2354, https://doi.org/10.5194/bg-21-2335-2024, 2024.

Hartmann, J., West, A. J., Renforth, P., Köhler, P., De La Rocha, C. L., Wolf-Gladrow, D. A., Dürr, H. H., and Scheffran, J.: Enhanced chemical weathering as a geoengineering strategy to reduce atmospheric carbon dioxide, supply nutrients, and mitigate ocean acidification, Reviews of Geophysics, 51, 113–149, https://doi.org/10.1002/rog.20004, 2013.

Hartmann, J., Suitner, N., Lim, C., Schneider, J., Marín-Samper, L., Arístegui, J., Renforth, P., Taucher, J., and Riebesell, U.: Stability of alkalinity in ocean alkalinity enhancement (OAE) approaches – consequences for durability of CO_2 storage, Biogeosciences, 20, 781–802, https://doi.org/10.5194/bg-20-781-2023, 2023.

He, J. and Tyka, M. D.: Limits and CO_2 equilibration of near-coast alkalinity enhancement, Biogeosciences, 20, 27–43, https://doi.org/10.5194/bg-20-27-2023, 2022.

Ho, D. T., Bopp, L., Palter, J. B., Long, M. C., Boyd, P. W., Neukermans, G., and Bach, L. T.: Monitoring, reporting, and verification for ocean alkalinity enhancement, State of the Planet, 2-oae2023, 1–12, https://doi.org/10.5194/sp-2-oae2023-12-2023, 2023.

Junger, P. C., Kavagutti, V. S., Deutschmann, I. M., Gazulla, C. R., Huber, P., Menezes, M., Paranhos, R., Amado, A. M., Ferrera, I., Rigonato, J., Chaffron, S., Gasol, J. M., Logares, R., and Sarmento, H.: Ecological Processes Shaping Marine Microbial Assemblages Diverge Between Equatorial and Temperate Time-Series, Molecular Ecology, 35, e70241, https://doi.org/10.1111/mec.70241, 2026.

K Grasshoff: Methods of seawater analysis, https://doi.org/10.1002/9783527613984, 1983.

Kapp, E. M.: The precipitation of calcium and magnesium from sea water by sodium hydroxide, The Biological Bulletin, 55, 453–458, https://doi.org/10.2307/1536800, 1928.

https://doi.org/10.5194/egusphere-2026-6827
Preprint. Discussion started: 19 November 2026
© Author(s) 2026. CC BY 4.0 License.

Kheshgi, H. S.: Sequestering atmospheric carbon dioxide by increasing ocean alkalinity, Energy, 20, 915–922, https://doi.org/10.1016/0360-5442(95)00035-F, 1995.

Kousoulas, K., Ferderer, A., Eriksen, R., and Bach, L. T.: Winners and losers under hydroxide-based ocean alkalinity enhancement in a Tasmanian plankton community, Journal of Phycology, 61, 989–1006, https://doi.org/10.1111/jpy.70052, 2025.

Kozlowski, J. A., Price, J., and Stein, L. Y.: Revision of N_2O-producing pathways in the ammonia-oxidizing bacterium Nitrosomonas europaea ATCC 19718, Applied and Environmental Microbiology, 80, 4930–4935, https://doi.org/10.1128/AEM.01061-14, 2014.

Lee, K., Kim, T.-W., Byrne, R. H., Millero, F. J., Feely, R. A., and Liu, Y.-M.: The universal ratio of boron to chlorinity for the North Pacific and North Atlantic oceans, Geochimica et Cosmochimica Acta, 74, 1801–1811, https://doi.org/10.1016/j.gca.2009.12.027, 2010.

Liu, H., Huang, L., Song, X., and Zhong, Y.: Using primary productivity as an index of coastal eutrophication: a case study in Daya Bay, Water and Environment Journal, 26, 235–240, https://doi.org/10.1111/j.1747-6593.2011.00281.x, 2012.

Liu, Y., Wang, X., Niu, R., Huang, X., Zhou, X., Li, H., Li, G., Hopwood, M. J., and Hou, S.: Resilience to Alkalinity Perturbation Reveals Ecosystem Stability under Ocean Alkalinity Enhancement, Ocean-Land-Atmosphere Research, 0, https://doi.org/10.34133/olar.0157, 2026.

Long, J. S., Hu, C., Robbins, L. L., Byrne, R. H., Paul, J. H., and Wolny, J. L.: Optical and biochemical properties of a southwest Florida whiting event, Estuarine, Coastal and Shelf Science, 196, 258–268, https://doi.org/10.1016/j.ecss.2017.07.017, 2017.

Louca, S., Parfrey, L. W., and Doebeli, M.: Decoupling function and taxonomy in the global ocean microbiome, Science, 353, 1272–1277, https://doi.org/10.1126/science.aaf4507, 2016.

Lueker, T. J., Dickson, A. G., and Keeling, C. D.: Ocean pCO_2 calculated from dissolved inorganic carbon, alkalinity, and equations for $K1$ and $K2$: validation based on laboratory measurements of CO_2 in gas and seawater at equilibrium, Marine Chemistry, 70, 105–119, https://doi.org/10.1016/S0304-4203(00)00022-0, 2000.

Martin, M.: Cutadapt removes adapter sequences from high-throughput sequencing reads, EMBnet. journal, 17, 10–12, https://doi.org/10.14806/ej.17.1.200, 2011.

McMurdie, P. J. and Holmes, S.: phyloseq: an R package for reproducible interactive analysis and graphics of microbiome census data, PloS one, 8, e61217, https://doi.org/10.1371/journal.pone.0061217, 2013.

McNichol, J., Berube, P. M., Biller, S. J., and Fuhrman, J. A.: Evaluating and improving small subunit rRNA PCR primer coverage for bacteria, archaea, and eukaryotes using metagenomes from global ocean surveys, Msystems, 6, 10.1128/msystems.00565-21, 2021.

Moras, C. A., Bach, L. T., Cyronak, T., Joannes-Boyau, R., and Schulz, K. G.: Ocean alkalinity enhancement – avoiding runaway $CaCO_3$ precipitation during quick and hydrated lime dissolution, Biogeosciences, 19, 3537–3557, https://doi.org/10.5194/bg-19-3537-2022, 2022.

https://doi.org/10.5194/egusphere-2026-6827
Preprint. Discussion started: 19 November 2026
© Author(s) 2026. CC BY 4.0 License.

Oksanen, J., Simpson, G. L., Blanchet, F. G., Kindt, R., Legendre, P., Minchin, P. R., O'hara, R. B., Solymos, P., Stevens, M. H. H., and Szoecs, E.: vegan: Community ecology package (2.6-4), Vienna (Austria): R Foundation for Statistical Computing, https://doi.org/10.32614/CRAN.package.vegan, 2022.

Ouyang, Z., Chen, R., Liu, Q., He, L., Cai, W.-J., and Yin, K.: Biological regulation of carbonate chemistry during diatom growth under different concentrations of Ca2+ and Mg2+, Marine Chemistry, 203, 38–48, https://doi.org/10.1016/j.marchem.2018.04.002, 2018.

Pan, Y., Li, Y., Chen, C.-T. A., Jiang, Z.-P., Cai, W.-J., Shen, Y., Ding, Z., Chen, Q., Di, Y., Fan, W., Zhu, C., and Chen, Y.: Unveiling the secrets of diatom-mediated calcification: Implications for the biological pump, Sci. China Earth Sci., 67, 2895–2909, https://doi.org/10.1007/s11430-023-1369-2, 2024.

Paul, A. J., Haunost, M., Goldenberg, S. U., Hartmann, J., Sánchez, N., Schneider, J., Suitner, N., and Riebesell, U.: Ocean alkalinity enhancement in an open-ocean ecosystem: biogeochemical responses and carbon storage durability, Biogeosciences, 22, 2749–2766, https://doi.org/10.5194/bg-22-2749-2025, 2025.

Perez, F. F. and Fraga, F.: A precise and rapid analytical procedure for alkalinity determination, Marine Chemistry, 21, 169–182, https://doi.org/10.1016/0304-4203(87)90037-5, 1987.

Pierrot, D., Epitalon, J.-M., Orr, J.C., Lewis, E., and Wallace, D. W. R.: MS Excel Program Developed for CO_2 System Calculations – Version 3.0, available at: https://github.com/dpierrot/co2sys_xl, 2021.

Quast, C., Pruesse, E., Yilmaz, P., Gerken, J., Schweer, T., Yarza, P., Peplies, J., and Glöckner, F. O.: The SILVA ribosomal RNA gene database project: improved data processing and web-based tools, Nucleic acids research, 41, D590–D596, https://doi.org/10.1093/nar/gks1219, 2012.

Ramírez, L., Pozzo-Pirotta, L. J., Trebec, A., Manzanares-Vázquez, V., Díez, J. L., Arístegui, J., Riebesell, U., Archer, S. D., and Segovia, M.: Ocean alkalinity enhancement (OAE) does not cause cellular stress in a phytoplankton community of the subtropical Atlantic Ocean, Biogeosciences, 22, 1865–1886, https://doi.org/10.5194/bg-22-1865-2025, 2025.

Renforth, P. and Henderson, G.: Assessing ocean alkalinity for carbon sequestration, Reviews of Geophysics, 55, 636–674, https://doi.org/10.1002/2016RG000533, 2017.

Riebesell, U., Basso, D., Geilert, S., Dale, A. W., Kreuzburg, M., and Meysman, F.: Mesocosm experiments in ocean alkalinity enhancement research, State of the Planet Discussions, 1–21, https://doi.org/10.5194/sp-2023-11, 2023.

Ringham, M., Hirtle, N., Shaw, C., Lu, X., Herndon, J., Carter, B., and Eisaman, M.: A comprehensive assessment of electrochemical ocean alkalinity enhancement in seawater: kinetics, efficiency, and precipitation thresholds, EGUsphere, 2024, 1–22, https://doi.org/10.5194/egusphere-2024-108, 2024.

Rognes, T., Flouri, T., Nichols, B., Quince, C., and Mahé, F.: VSEARCH: a versatile open source tool for metagenomics, PeerJ, 4, e2584, https://doi.org/10.7717/peerj.2584, 2016.

Sánchez, N., Goldenberg, S. U., Brüggemann, D., Jaspers, C., Taucher, J., and Riebesell, U.: Plankton food web structure and productivity under ocean alkalinity enhancement, Science Advances, 10, https://doi.org/10.1126/sciadv.ado0264, 2024.

https://doi.org/10.5194/egusphere-2026-6827
Preprint. Discussion started: 19 November 2026
© Author(s) 2026. CC BY 4.0 License.

Schulz, K. G., Bach, L. T., and Dickson, A. G.: Seawater carbonate chemistry considerations for ocean alkalinity enhancement research: theory, measurements, and calculations, State of the Planet, 2-oae2023, 1–14, https://doi.org/10.5194/sp-2-oae2023-2-2023, 2023.

Song, X., Huang, L., Zhang, J., Huang, X., Zhang, J., Yin, J., Tan, Y., and Liu, S.: Variation of phytoplankton biomass and primary production in Daya Bay during spring and summer, Marine Pollution Bulletin, 49, 1036–1044, https://doi.org/10.1016/j.marpolbul.2004.07.008, 2004.

Stanton, C., Barnes, B. D., Kump, L. R., and Cosmidis, J.: A re-examination of the mechanism of whiting events: A new role for diatoms in Fayetteville Green Lake (New York, USA), Geobiology, 21, 210–228, https://doi.org/10.1111/gbi.12534, 2023.

Subhas, A. V., Marx, L., Reynolds, S., Flohr, A., Mawji, E. W., Brown, P. J., and Cael, B. B.: Microbial ecosystem responses to alkalinity enhancement in the North Atlantic Subtropical Gyre, Front. Clim., 4, https://doi.org/10.3389/fclim.2022.784997, 2022.

Suitner, N., Faucher, G., Lim, C., Schneider, J., Moras, C. A., Riebesell, U., and Hartmann, J.: Ocean alkalinity enhancement approaches and the predictability of runaway precipitation processes: results of an experimental study to determine critical alkalinity ranges for safe and sustainable application scenarios, Biogeosciences, 21, 4587–4604, https://doi.org/10.5194/bg-21-4587-2024, 2024.

Suitner, N., Hartmann, J., Varliero, S., Faucher, G., Suessle, P., and Moras, C. A.: Surface area and Ω-aragonite oversaturation as controls of the runaway precipitation process in ocean alkalinity enhancement, Biogeosciences, 23, 3965–3980, https://doi.org/10.5194/bg-23-3965-2026, 2026.

Sun, C.-C., Wang, Y.-S., Wu, M.-L., Dong, J.-D., Wang, Y.-T., Sun, F.-L., and Zhang, Y.-Y.: Seasonal Variation of Water Quality and Phytoplankton Response Patterns in Daya Bay, China, International Journal of Environmental Research and Public Health, 8, 2951–2966, https://doi.org/10.3390/ijerph8072951, 2011.

Sun, W., Jayaraman, S., Chen, W., Persson, K. A., and Ceder, G.: Nucleation of metastable aragonite $CaCO_3$ in seawater, Proceedings of the National Academy of Sciences, 112, 3199–3204, https://doi.org/10.1073/pnas.1423898112, 2015.

Tammen, J. K., Kittu, L. R., Schartau, M., Faucher, G., Schulz, K. G., Boersma, M., and Riebesell, U.: Spring phytoplankton bloom dynamics reveal thresholds of ocean alkalinity enhancement in the North Sea, Commun Earth Environ, 7, 750, https://doi.org/10.1038/s43247-026-03986-y, 2026.

Team, R. C.: R: A Language and Environment for Statistical Computing. R Foundation for Statistical Computing, Vienna, Austria. https://www.R-project.org/, 2023.

Tesson, B., Gaillard, C., and Martin-Jézéquel, V.: Brucite formation mediated by the diatom Phaeodactylum tricornutum, Marine Chemistry, 109, 60–76, https://doi.org/10.1016/j.marchem.2007.12.005, 2008.

Tian, M., Hartmann, J., Suitner, N., Amann, T., Kempe, S., Lim, C., and Moras, C. A.: Stability of alkalinity in the land-ocean transition zone: a geochemical CDR perspective for the Elbe River, Germany, Environ. Res. Lett., 20, 094053, https://doi.org/10.1088/1748-9326/adeeab, 2025.

https://doi.org/10.5194/egusphere-2026-6827
Preprint. Discussion started: 19 November 2026
© Author(s) 2026. CC BY 4.0 License.

Wang, B., Chen, M., Zheng, M., and Qiu, Y.: The biological uptake of dissolved iron in the changing Daya Bay, South China Sea: Effect of pH and DO, Marine Pollution Bulletin, 178, 113635, https://doi.org/10.1016/j.marpolbul.2022.113635, 2022.

Wang, X., Li, H., Zheng, C., Yang, J., Zhang, Y., Zhang, M., Qi, Z., Xiao, K., and Zhang, X.: Submarine groundwater discharge as an important nutrient source influencing nutrient structure in coastal water of Daya Bay, China, Geochimica et Cosmochimica Acta, 225, 52–65, https://doi.org/10.1016/j.gca.2018.01.029, 2018.

Wang, Z., Qi, Y., Chen, J., Xu, N., and Yang, Y.: Phytoplankton abundance, community structure and nutrients in cultural areas of Daya Bay, South China Sea, Journal of Marine Systems, 62, 85–94, https://doi.org/10.1016/j.jmarsys.2006.04.008, 2006.

Welschmeyer, N. A.: Fluorometric analysis of chlorophyll a in the presence of chlorophyll b and pheopigments, Limnology and Oceanography, https://doi.org/10.4319/lo.1994.39.8.1985, 1994.

Wurgaft, E., Wang, Z. A., Churchill, J. H., Dellapenna, T., Song, S., Du, J., Ringham, M. C., Rivlin, T., and Lazar, B.: Particle Triggered Reactions as an Important Mechanism of Alkalinity and Inorganic Carbon Removal in River Plumes, Geophysical Research Letters, 48, e2021GL093178, https://doi.org/10.1029/2021GL093178, 2021.

Xin, X., Goldenberg, S. U., Taucher, J., Stuhr, A., Arístegui, J., and Riebesell, U.: Resilience of Phytoplankton and Microzooplankton Communities under Ocean Alkalinity Enhancement in the Oligotrophic Ocean, Environ. Sci. Technol., https://doi.org/10.1021/acs.est.4c09838, 2024.

Xin, X., Liu, Y., Chang, R., Lei, R., Zhu, M., Wang, X., Wang, X. C., and Liu, J.: Biogeochemical responses to ocean alkalinity enhancement in the North China Sea, EGUsphere, 1–13, https://doi.org/10.5194/egusphere-2026-5281, 2026.

Yang, X., Tan, Y., Li, K., Zhang, H., Liu, J., and Xiang, C.: Long-term changes in summer phytoplankton communities and their influencing factors in Daya Bay, China (1991–2017), Marine Pollution Bulletin, 161, 111694, https://doi.org/10.1016/j.marpolbul.2020.111694, 2020.

Yeh, Y.-C., McNichol, J., Needham, D. M., Fichot, E. B., Berdjeb, L., and Fuhrman, J. A.: Comprehensive single-PCR 16S and 18S rRNA community analysis validated with mock communities, and estimation of sequencing bias against 18S, Environmental Microbiology, 23, 3240–3250, https://doi.org/10.1111/1462-2920.15553, 2021.

Zhang, H., Cheng, W., Chen, Y., Shi, Z., Gong, W., and Liu, S.: Importance of large-scale coastal circulation on bay-shelf exchange and residence time in a subtropical embayment, the northern South China Sea, Ocean & Coastal Management, 168, 72–89, https://doi.org/10.1016/j.ocecoaman.2018.10.033, 2019.

Zhang, L., Lei, S., Lyu, S., Bian, H., Chen, J., Ren, H., Su, B., Hu, Y., Zheng, L., and Liu, J.: Site-specific seawater conditions modulate bacterial community responses to ocean alkalinity enhancement, Marine Pollution Bulletin, 233, 120391, https://doi.org/10.1016/j.marpolbul.2026.120391, 2026.

Zhou, J., Zheng, Y., Hou, L., Qi, L., Mao, T., Yin, G., and Liu, M.: Nitrogen input modulates the effects of coastal acidification on nitrification and associated N2O emission, Water Research, 261, 122041, https://doi.org/10.1016/j.watres.2024.122041, 2024.